Energy Management for Multiple-Pulse Missiles

Craig Phillips*
Naval Surface Warfare Center, Dahlgren, Virginia 22448

This paper examines maximum final speed and minimum flight-time trajectories of missiles that have two- or three-pulse rockets for both horizontal and vertical plane flight. The optimal rocket-propellant loadouts and pulse ignition times are determined using parameter optimization coupled with explicit solution of the trajectories. The results indicate that the three-pulse configuration is superior for both problems in horizontal flight and that it matches the performance of an ideal boost-sustain motor. For vertical plane flight, the two-pulse motor is superior to a boost-only motor. The three-pulse motor does not produce a significant practical improvement in performance for vertical plane flight beyond that of the two-pulse motor.

Introduction

THE development of practical designs for pulsed solid rocket motors has opened new avenues for the control of missile trajectories. To effectively utilize this new technology, techniques must be developed to optimize the trajectories and pulse motor designs. The present paper seeks to create a method to rapidly optimize pulse rocket-motor designs and trajectories and to determine the applicability of pulse motors to a spectrum of missile missions with an emphasis on the surface-to-air missile.

The seminal works in the field of rocket-thrust and rocket-motor design optimization used the calculus of variations to demonstrate that the continuously throttleable ideal boost-sustain motor maximized missile performance.[1,2] The requirement of the use of fixed nozzle designs in actual rocket-motor designs prevented these theoretical performance limits from being achieved. The practical boost-sustain motor suffers a specific impulse degradation in both the boost and sustain portions of the thrust history with the greatest losses in the low-burn-rate sustain phase. The pulse rocket motor allows the use of nearly constant mass flow rate during operation, which gives a 5–7% advantage in overall specific impulse over the practical boost-sustain motor. Through proper design of the motor and control algorithms, the pulsed rocket motor is able to approach the theoretical limits set for the ideal boost-sustain motor. Thus, the pulse motor should offer performance improvement over the practical boost-sustain motor.

The complete solution to the optimal pulse motor problem involves simultaneous optimization of the motor parameters, ignition times, and trajectory shaping. Two broad approaches are available for solution of this problem. The first is the optimal control methodology, which yields a two-point boundary value problem. The resulting problem can be solved numerically using an open-loop solution for both the motor design and the missile guidance. Another method to solve the optimal control problem is to approximate the system by a reduced-order model and to find the corresponding closed-loop analytical guidance and ignition law. While yielding an implementable algorithm, this method involves approximations which may not be appropriate. In addition, the reduced-order analytical solutions do not address the selection of the pulse motor design parameters.

Presented as Paper 88-0334 at the AIAA 26th Aerospace Sciences Meeting, Reno, NV, Jan. 7–11, 1988; received Nov. 19, 1987; revision received March 15, 1990.

*Aerospace Engineer, Weapon Systems Department.

The reduced-order approach to obtain an analytical solution has been used by a number of authors. This approach has been used with success to determine pulse ignition laws to minimize time of flight and to maximize final speed during horizontal flight[3,4,5] of an air-to-air missile. The problem of ignition of the second pulse and trajectory shaping in the vertical plane to minimize the time of flight has been addressed by reduced-order approximations for an air-to-air missile[6] and for a surface-to-surface missile.[4] The use of model reduction in these solutions contributes to uncertainty as to their optimality for the complete problem.

The other approach to the solution of the complete problem is parameter optimization. In this approach the optimal control is approximated by an optimal finite set of parameters. This method has been used to determine the range maximal motor parameters and open-loop trajectory shaping of a two-pulse air-to-surface missile.[7] In that work the solution was subject to minimum dynamic pressure and average speed constraints for the high-altitude mission and a maximum altitude limit for the low-altitude mission.

Although the resulting open-loop trajectory shaping and pulse ignition schedule from the parameter optimization are not directly implementable in a real-time system, such an approach remains a valuable tool. During the conceptual design phase, it can be used to quickly determine the applicability of the pulse rocket motor for each candidate design and mission. By developing the open-loop optimal trajectory shaping and motor design, the maximum performance for each design can be determined independent of the guidance scheme, which is likely to be unspecified at the conceptual stage of the design. Thus, the motor specifications that enhance the mission can be created early in the program. Second, the resulting maximum possible performance determined by this method provides a benchmark against which reduced-order analytical and implementable guidance and pulse ignition laws may be evaluated. A third possibility has recently appeared in that the open-loop optimal control for guidance and ignition control may be modeled in a polynomial network to become an implementable control algorithm.[8]

The present study develops a parameter optimization approach to determine the motor design and trajectory shaping for the two problems of maximizing final speed and minimizing the flight time as applied to an air-to-air missile in horizontal flight and a surface-to-air missile in vertical plane flight. This method can then be used to evaluate the effectiveness of the pulse motor for the missions considered.

Although similar in many aspects to previous work and particularly to that of Ref. 7, the present work offers several new contributions. That reference dealt with the different problem of range maximization of an air-to-surface missile with significantly different operational conditions. Previously published work with both the optimal control and parameter

optimization approaches has been limited to two pulses whereas the present work considers the benefits of the three-pulse motor. The results demonstrate that the three-pulse motor can effectively reproduce the performance of the continuously throttleable ideal boost-sustain motor for the horizontal flight problem. The present work demonstrates for the first time that the three-pulse motor improves the final speed for the vertical problem over that of the one- and two-pulse motors. In addition, for minimal time vertical plane flight, the two-pulse motor is shown to reduce the flight time whereas the three-pulse motor only reproduces the two-pulse results.

Also, the present results are used to verify the optimality of the reduced-order analytical pulse ignition laws for the horizontal flight minimal time and maximum final speed problems.[3,4,5] The robustness of the minimal time ignition law is considered. The conclusion of Ref. 4 that the pulse motor is not advantageous for vertical plane minimum time flight is shown to be incorrect by a counterexample.

Missile Modeling

This section describes an overview of the model of the missile used in this study with additional details available in the Appendix. The missile is modeled as a point mass above a flat nonrotating Earth and constrained to fly in a vertical plane. The four states modeled include the specific energy, the altitude, the range, and the flight-path angle. The mass properties and airframe are representative of modern surface-to-air missiles. The aerodynamic data are expressed in terms of a cubic spline of drag coefficient as a function of lift coefficient and Mach number. The maximum lift coefficient corresponding to the maximum angle of attack is modeled with a cubic spline as a function of Mach number.

An important area of the modeling is the thrust and mass history. The pulse motor thrust history is modeled as a series of constant sea level thrust pulses. The effect of pressure thrust is included in the modeling, so that delivered thrust is a function of altitude. The thrust is assumed to lie along the velocity axis. A constant burn-rate motor was used to maximize the delivered specific impulse and to avoid the empirical correction to the specific impulse associated with the modeling of variable burn-rate motors. Since the burn rate and sea level thrust used in this study were fixed, the vehicle weight is a linear function of total burn time. The sea level specific impulse was fixed throughout the study with the effect of expended inert mass modeled as a reduction in its value.

Trajectory and Motor Optimization

The description of the horizontal flight optimization problems will be presented first to be followed by the vertical plane problems that have increased dimensionality. The horizontal flight problems involve the selection of the control and motor parameters, which maximize the final speed at a specified final range and free final time t_f or which minimize the flight time to this same range. The initial and final conditions for these problems are given in Table 1. For both the horizontal and vertical plane problems, the parameters available for optimization include t_f and the motor parameters. The flight time is included as a parameter because it is used as the termination criterion for the trajectory model.

Each motor configuration has a different number of motor related design parameters. For the three-pulse motor, there are four motor parameters: 1) the propellant fraction in the first pulse, 2) the fraction of remaining propellant allocated to the second pulse, 3) the fraction of the total flight time used during the first ignition delay, and 4) the fraction of the total time remaining after burnout of the second pulse to be used in the second ignition delay.

Table 1 Initial and final conditions for horizontal flight problems

Initial speed (ft/s)	567
Altitude (ft)	20,000
Initial weight (lb)	976
Final weight (lb)	545
Final range (ft)	150,000

Table 2 Initial and final conditions for vertical plane flight problems

Initial altitude (ft)	0
Initial speed (ft/s)	114
Launch angle (deg)	90
Initial weight (lb)	976
Final altitude (ft)	70,000
Final range (ft)	120,000
Final weight (lb)	545

The two-pulse motor has only two motor-related parameters: 1) the propellant fraction in the first pulse, and 2) the fraction of total flight time spent in the ignition delay. The one-pulse motor has no parameters available for optimization. The specified final range determines the flight time for the one-pulse configuration for the horizontal flight problem.

The constraints on the horizontal flight problems serve both to define the problems and to keep the parameter values within physically realizable bounds. The only equality constraint is on the final range. Inequality constraints are used to maintain the ignition delays greater than zero. Also, an inequality constraint is used to ensure that burnout of the final pulse occurs before trajectory termination. Finally, the one-path constraint on the horizontal flight problems constitutes the upper limit on the magnitude of the lift coefficient. This constraint is converted into a terminal constraint by propagating the integral square violation of the lift coefficient constraint over the entire flight to the final time. The total accumulated violation is limited by an upper-bound inequality constraint with a magnitude selected to provide reasonable performance.[9]

The optimization approach for the vertical plane problems is now discussed. The problems considered include flight to a specified range and altitude with the maximum final speed and free t_f, the minimum flight time, and the maximum final speed with a maximum constraint on t_f. The initial and final conditions are given in Table 2. The flight-time parameter t_f is used as the termination criterion as with the horizontal flight scenarios. In addition, the pulse motor parameters are identical with those of the horizontal flight problems.

In addition to these parameters, the vertical plane problems have design parameters to control the shaping of the trajectory. For this model, the load factor history is directly parameterized as a multisegment linear function with t_f-normalized flight time as the independent variable. The load factor values at the node points are then included in the optimization parameter set. The number of nodes was set at five with normalized time locations of 0.0, 0.25, 0.5, 0.75, and 1. Early in this study, the variation in missile performance with the number of load factor nodes was investigated with five providing good performance.

Constraints for the vertical plane flight problems include two equality constraints on the final altitude and range as given in Table 2. The motor-related constraints defined previously are applied to these problems. The integral square penalty is used to enforce the path constraint on the lift coefficient. A minimum dynamic pressure inequality path constraint was also enforced by a different approach. During the trajectory the lowest value of the dynamic pressure was tracked. The resulting value was then enforced to be greater than the minimum dynamic pressure bound by a terminal inequality constraint. For the time-constrained maximum final speed trajectories, an upper bound inequality constraint was placed on the value of t_f.

In the present work, a quasi-Newton method with constraint projection is used for parameter optimization. The Kelley-Speyer algorithm[10] minimizes a scalar-valued function $f(x)$ (where x is an n vector) subject to m equality and p inequality constraints:

$$g_j = 0, \qquad j = 1,\ldots, m$$

$$g_j \geq 0, \qquad j = m+1,\ldots, m+p$$

The optimization process conducts a one-dimensional search along the projected gradient vector in order to minimize the function $f + g\lambda$. The search is conducted in terms of the scalar variable α so that the search step is defined as

$$\Delta x = -\alpha H(f_x + g_x\lambda)$$

where

$$\lambda = -(g_x{}^T H g_x)^{-1} g_x{}^T H f_x$$

The terms g_x and f_x are the constraint and function gradients.

The dimensions of g and λ are determined by the active-constraint set screening logic. The matrix H is an approximation to the inverse of the Hessian matrix and approaches the true value at convergence. The one-dimensional search is terminated upon reaching a minimum as determined by user input tolerances or if the constraint violations exceed a prescribed tolerance.

During the optimization cycle, the H matrix is updated in such a manner as to maintain positive definiteness by the Broyden-Fletcher-Goldfarb-Shanno update algorithm first described in Ref. 11.

Projection algorithms require one or more correction cycles after an optimization cycle. Thus, the algorithm cycles between optimization and correction cycles as controlled by user-specified tolerances until the projected gradient meets a prescribed tolerance and near-quadratic convergence is achieved.

Although the quasi-Newton methods coupled with explicit solution of the dynamics have been used extensively, promising efforts to optimize missile trajectories using sequential quadratic programming with collocation methods have been reported.[12]

Horizontal Flight

The horizontal flight problem considered is that of a missile which must fly at a constant altitude from a nonzero initial speed to a specified final range. The problems of minimizing the flight time t_f and maximizing the final speed are both analyzed.

The set of parameter values that maximize the final speed at the specified downrange are given in Table 3. The final speed and average speed for each configuration are given in Table 4. The corresponding velocity histories are given in Figs. 1-3.

Table 3 Parameter values for maximum V_f horizontal flight

	Fuel fractions Pulse no.			Ignition delay (s) Pulse no.		
Motor	1	2	3	2	3	t_f (s)
Single	1.0	—	—	—	—	72.5
Double	0.53	0.47	—	108.3	—	121.8
Triple	0.26	0.18	0.55	63.9	62.3	139.6

Table 4 Final values for maximum V_f horizontal flight

	Single pulse	Double pulse	Triple pulse
Speed (ft/s)	1025	2694	3143
Average speed (ft/s)	2069	1232	1074

The use of multiple pulses avoids the high-peak speeds and drag of the boost-only missile during the immediate postboost period. This reduces the total drag impulse during the flight and yields significant increases in the final speed. The two-pulse motor produced a 163% increase in final speed over the boost-only motor while the three-pulse motor produced a 206% increase. The increase in final speed comes at the cost of significantly reduced average speed with the three-pulse motor having a 48% reduction in average speed.

The improvement in performance as the number of pulses increased may be understood by examining the maximum final

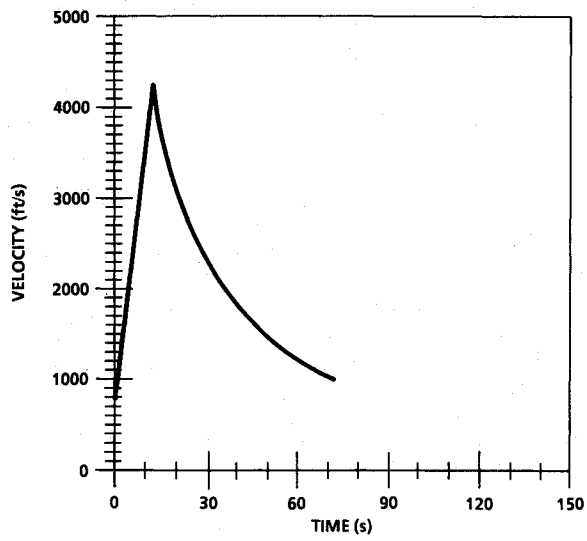

Fig. 1 Boost-only velocity history.

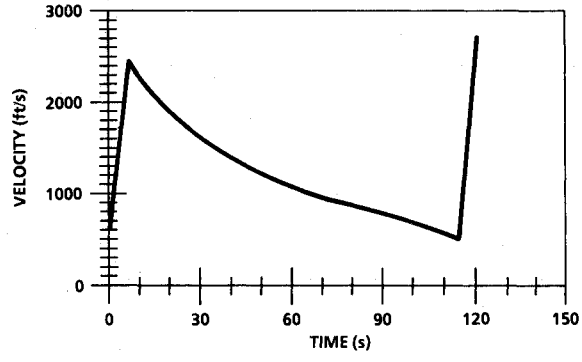

Fig. 2 Two-pulse horizontal velocity history.

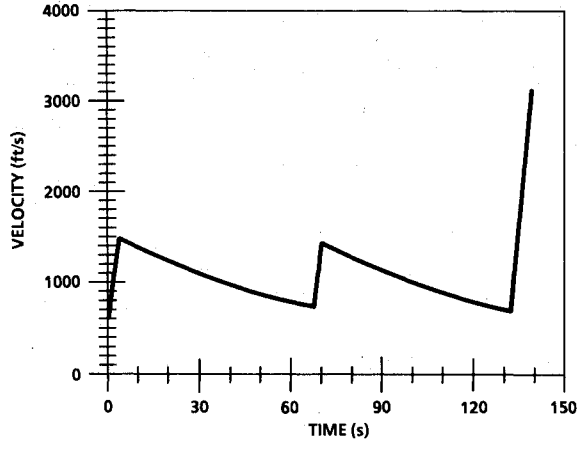

Fig. 3 Three-pulse horizontal velocity history.

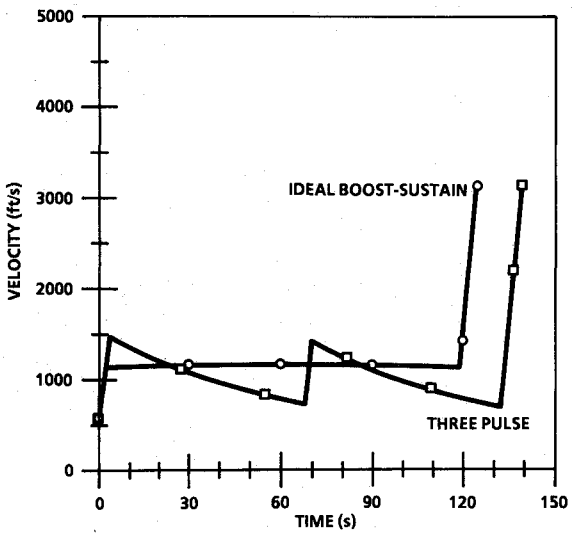

Fig. 4 Comparison of pulse and boost-sustain velocities.

speed performance of the continuously throttleable ideal boost-sustain motor described by Hibbs.[1] The final speed maximizing thrust history involves an initial maximum thrust segment until intersection with the singular arc defined in terms of the mass and speed. The singular control is followed until fuel is exhausted or the endpoint is reached at which point all remaining fuel is burned at the maximum rate.

The singular control consists of a program relating the optimal speed for the missile to fly as a function of its mass. In terms of normalized velocity and normalized mass, this relationship, from Ref. 1, is

$$\bar{m}^2 = \bar{V}^4 (\bar{V}+1)(\bar{V}+3)^{-1}$$

The normalized mass $\bar{m}$ and speed $\bar{V}$ are defined in terms of the flight conditions and airframe characteristics:

$$\bar{m} = \frac{2W}{V_e^2 \rho S (C_{D0}/k)}$$

$$\bar{V} = \frac{V}{V_e}$$

where C_{D0} and k are the zero-lift drag coefficient and the induced drag factor used for the drag polar. The weight is given by W, the exhaust velocity by V_e, the reference area by S, and the atmospheric density by ρ.

The singular arc determines both the velocity and thrust history for the continuously throttleable ideal boost-sustain motor. The speed determined by this relation is one which will minimize the energy loss per unit of range. The velocity history and performance for the ideal boost-sustain motor used with the missile of this study was determined by approximating the aerodynamic drag data with a drag polar. The resulting velocity history is compared to that of the three-pulse motor in Fig. 4.

The three-pulse motor drives the missile at an average speed that is biased slightly less than that of the ideal boost-sustain motor. To keep the average drag impulse per unit range close to the ideal boost-sustain singular arc velocity history, the average speed of the pulse motor must be slightly lower to counteract the effects of the quadratic speed dependence of the drag during the peaks. It would be reasonable to project that increasing the number of pulses in the motor would allow the ideal boost-sustain velocity history to be even more closely approximated. In terms of the goal of maximizing final speed, this is unnecessary, as the three-pulse motor matches the performance of the theoretical boost-sustain motor.

Table 5 Parameter values for minimal time horizontal flight

	Fuel fractions Pulse no.			Ignition delay (s) Pulse no.		
Motor	1	2	3	2	3	t_f (s)
Single	1.0	—	—	—	—	72.5
Double	0.73	0.27	—	18.6	—	70.4
Triple	0.66	0.18	0.16	11.7	10.6	70.3

Table 6 Postboost and final speed comparisons

	Postboost speed, ft/s	Final speed, ft/s
Double min t_f	3190	1269
Double max V_f	2470	2694
Triple min t_f	2948	1297
Triple max V_f	1482	3142

It is reasonable to assume that a pulse ignition algorithm could be based on the ratio of velocity to drag. Such an algorithm has been developed analytically[3,5] for an approximate model. In this method the second pulse is ignited when the following condition is satisfied:

$$V(t_i)/D(t_i) = C_m V(t_{i+1})/D(t_{i+1})$$

where the left-hand side is the current velocity to drag ratio and the right-hand side represents the estimated velocity to drag ratio after a constant mass impulsive burn multiplied by a mass correction term C_m.

To test the validity of this algorithm, it was used to determine the second pulse ignition time of the maximum final speed two-pulse motor design previously developed. The pulse ignition time determined by this algorithm agreed exactly with the value determined by the parameter optimization technique that is presented in Table 3. Thus, this ignition law will maximize the final speed for a fixed two-pulse motor design.

The second horizontal flight problem considered was that of determining the pulse motor parameters and pulse ignition times that minimized the time of flight to a specified range. This is the equivalent of maximizing the average speed over the flight. This problem was analyzed with the same initial and final conditions as the maximum final speed problem previously presented. The relative ability of each motor configuration to minimize the flight time will be discussed as will be the ability of the maximum average speed pulse ignition law of Ref. 4.

The minimum time pulse motor parameters for the two- and three-pulse motor configuration are given in Table 5. The one-pulse motor parameters are fixed but are included in the table. For the minimal time solution, the fuel fraction allotted to the initial pulse is greatly increased as compared to the maximum final speed solution. In addition, the ignition delays are greatly reduced. The two- and three-pulse motors produce only small reductions in the flight time relative to the boost-only motor. For this scenario, the reduction in flight time between the two- and three-pulse motors would not warrant the use of the three-pulse motor.

The reduction in the flight time as compared to the maximum final speed trajectories comes at the cost of very high speed peaks at the boost pulse burnout and lowered final speeds. For the maximum final speed solutions, the maximum speed before the terminal pulse occurs at burnout of the initial boost pulse. A comparison between the two- and three-pulse minimal time and maximum final speed solution postboost and final speeds is given in Table 6. The three-pulse design allows greater performance in that it reduces this postboost speed while improving the final time of flight as compared to the two pulse. This is the consequence of the increased number of design variables available with the three-pulse design.

Just as for the maximum final speed case, an analytical ignition law has been developed for maximizing the average speed of pulsed missile in horizontal flight.[4,5] In this approach, the pulse is fired when the following condition is satisfied:

$$\frac{[V(t_i) - V(t_f)]}{D(t_i)} = \frac{[V(t_{i+1}) - V(t_f)]}{D(t_{i+1})}$$

where the V and D represent the velocity and drag and t_i is the present time. The term t_{i+1} is the time of pulse burnout should ignition occur at the present time.

It should be noted that the final velocity must be estimated for this algorithm. Unfortunately this introduces an aspect of open-loop control to the problem as this value must be determined iteratively and off-line of the implemented system. This aspect can lead to problems in terms of robustness in cases where the estimate of the final velocity is not accurate.

This algorithm was implemented with the minimal time two-pulse motor fuel allocation developed previously. The value of $V(t_f)$ as a function of the range-to-go for this particular study was determined by simulation and implemented in this algorithm. The condition for pulse ignition was exactly satisfied at the instant of pulse ignition as determined by the parameter optimization approach. Thus, this algorithm is a good tool for determining ignition time to minimize the flight time. The use of the impulsive burn rocket equation to estimate the burnout speed seems to be most appropriate for high-thrust vehicles.

The issue of robustness in the presence of errors in the estimate of the final velocity was considered. The minimal t_f fuel loadout previously determined for the nominal airframe was run with a 20% increase in the axial drag. The pulse delay that minimized the flight time was developed for the new airframe with this fuel allocation. This delay was compared to the ignition delay as determined by the ignition algorithm using final velocity data for the nominal airframe.

The minimum time pulse delay was 28.1 s whereas the ignition law yielded a delay of 23.3 s. The respective flight times were 80.4 and 80.6 s. The agreement between the flight times in spite of the difference in ignition times indicates a weak dependence on the ignition time. The error in the ignition time indicates that this algorithm exhibits some of the undesirable aspects of open-loop control.

Vertical Plane Flight

The techniques developed were extended to handle optimization of pulse rocket-motor trajectories in the vertical plane. Three problems were analyzed. The first considered maximizing the final speed at a specified altitude and range subject to the maximum lift coefficient and minimum dynamic pressure constraints. The second problem was to determine the minimal flight-time trajectory subject to these constraints. The one-, two-, and three-pulse motors were considered in both of these. A third problem of trading off flight time for final speed optimally through a maximum final time constraint was applied only to the two-pulse motor.

Table 7 Maximum final speed vertical plane parameter values

	Single pulse	Double pulse	Triple pulse
Fuel fraction			
First pulse	1.00	0.55	0.44
Second pulse	—	0.45	0.36
Third pulse	—	—	0.20
Ignition delay (s)			
Second pulse	—	28.3	13.7
Third pulse	—	—	82.0
The t_f (s)	64.8	75.1	109.6
Load factor spline			
1	−0.349	−0.810	−0.172
2	−3.410	−0.683	−0.788
3	−0.928	−0.136	−0.089
4	−0.446	−0.647	−0.004
5	−0.138	0.043	0.012

The maximum final speed parameter values are given in Table 7 for each of the three motor configurations. The final values are given in Table 8. The comparison of the trajectories and velocity histories for the one- and two-pulse configurations are given in Figs. 5 and 6. Figures 7 and 8 show the comparisons between the two- and three-pulse configurations.

The results yield some interesting observations about the maximum final speed trajectories. The three-pulse motor configuration achieves a very high loft and thus has the minimum dynamic pressure limit active in its solution. This constraint defines the upper limit of the apogee. The one- and two-pulse configurations have shallower trajectories without an active minimum dynamic pressure limit in the solutions.

The performance results indicate that both the two- and three-pulse motor configurations can increase the final speed of the missile relative to the boost-only configuration. The increase in final speed is not as dramatic as for the horizontal flight case because of the gravity penalty associated with lifting the unburned fuel to higher altitudes and the lower aerodynamic drag at higher altitudes. The two-pulse configuration

Table 8 Final values for maximum final speed trajectories

	Single pulse	Double pulse	Triple pulse
Final speed (ft/s)	2135	2500	2792
Avg. speed (ft/s)	1852	1598	1095
Path angle (deg)	−13.3	−2.3	−37.2

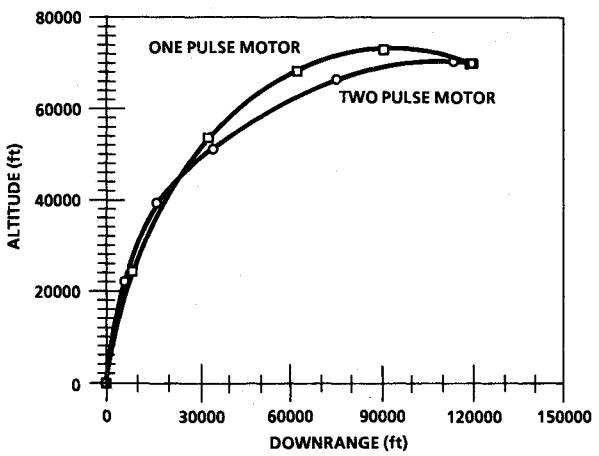

Fig. 5 One- and two-pulse vertical plane trajectories.

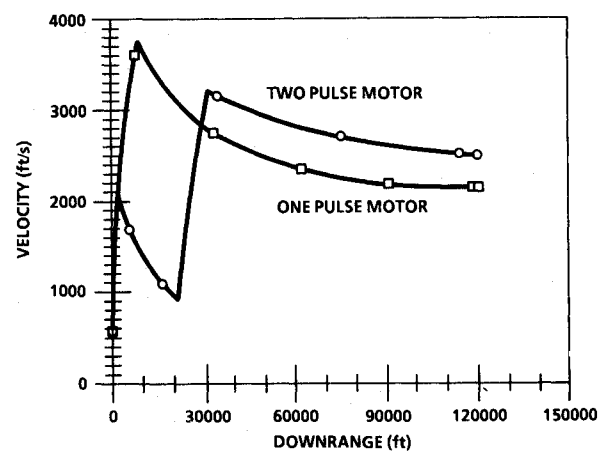

Fig. 6 One- and two-pulse vertical plane velocity histories.

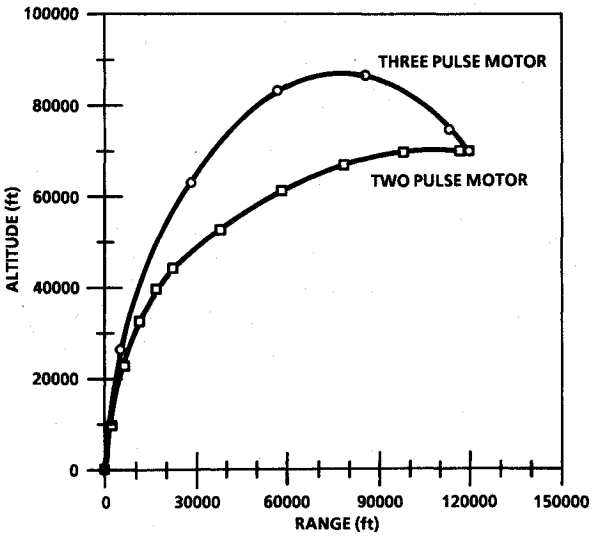

Fig. 7 Two- and three-pulse vertical plane trajectories.

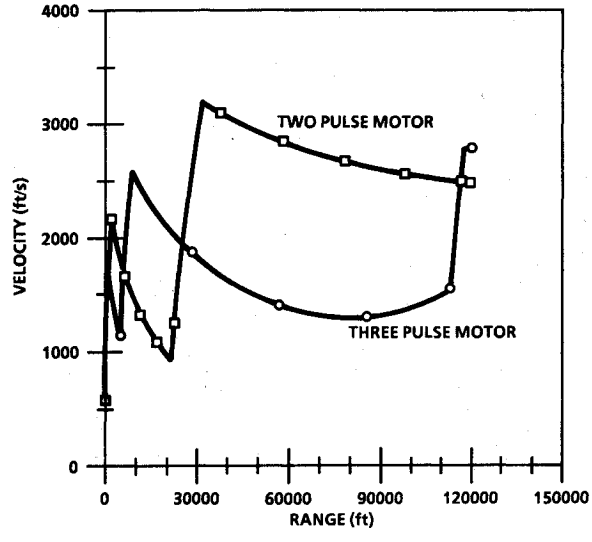

Fig. 8 Two- and three-pulse vertical plane velocity histories.

improved the final speed by 18% whereas the three pulse yielded a 30% increase over the nominal boost-only configuration. The two-pulse motor decreased the average ground speed by only a small amount whereas the three-pulse configuration greatly reduced the average speed because of its greater lofting.

The results for the time-minimal vertical plane flight are now discussed. The optimization algorithm was modified to minimize the flight time to the fixed target point. The time-minimal parameters are given in Table 9 with the final conditions given in Table 10.

The outstanding feature of these results is that the three-pulse motor duplicates the two-pulse motor trajectory and does not provide any additional benefits for the vertical plane time-minimal flight problem. The missile airframe chosen for this study is representative, so this conclusion may be applicable to a class of vehicles.

Another feature is that the two-pulse motor is superior to the one-pulse motor for the time-minimal problem in terms of the flight time and the final speed. The two-pulse motor uses a short ignition delay to avoid the high drag associated with high speeds at low altitudes. To further avoid this drag, the two-pulse configuration has a more vertical ascent through the dense atmosphere followed by a hard maneuver to lower the

Table 9 Time-minimal parameter values

	Single pulse	Double pulse	Triple pulse
Fuel fraction			
First pulse	1.00	0.60	0.59
Second pulse	—	0.40	0.36
Third pulse	—	—	0.05
Ignition delay (s)			
Second pulse	—	4.5	4.5
Third pulse	—	—	0.5
The t_f (s)	62.1	61.1	61.1
Load factor nodes			
1	−1.440	−1.340	−1.340
2	−2.850	−2.370	−2.360
3	−0.356	−0.581	−0.577
4	0.302	0.189	0.180
5	0.602	0.667	0.672

Table 10 Final conditions for time-minimal flight

	Single pulse	Double pulse	Triple pulse
Final speed (ft/s)	1970	2118	2119
Avg. speed (ft/s)	1932	1966	1966
Path angle (deg)	4.9	7.0	7.0

Table 11 Parameter values for time-constrained maximum final velocity trajectories

	t_f constraint (s)					
	Open	70	67	65	63	Min t_f
Boost pulse						
Fuel fraction	0.55	0.54	0.54	0.55	0.56	0.60
Delay (s)	28.3	21.4	17.5	14.4	10.9	4.5
Actual t_f (s)	75.1	70.0	67.0	65.0	63.0	61.1
Load factor node values						
1	−0.81	−0.89	−1.0	−1.1	−1.1	−1.3
2	−0.68	−0.65	−0.83	−1.0	−1.4	−2.4
3	−0.14	−0.78	−1.0	−1.1	−1.1	−0.6
4	−0.65	−0.63	−0.61	−0.58	−0.47	−0.19
5	0.04	0.02	0.01	0.01	0.02	0.67

flight-path angle to minimize the distance traveled to the target point.

The superiority of the two-pulse configuration conflicts with the conclusion drawn in Ref. 4 that the two-pulse motor is inferior to the boost-only motor in minimal time vertical plane flight. The reasoning in that reference is based upon the singular perturbation time scaling drawn from aircraft dynamics. Application of this time scaling to the rocket problem appears to be inappropriate as has been previously discussed by other authors.[5] Also, the conclusions of Ref. 6 indicate the superiority of the pulse motor over the boost-only motor for minimum time flight in the vertical plane.

The final problem considered in this study is the use of a pulse motor to tradeoff final speed and average speed. This extra control degree of freedom should allow the pulse motor to trade these two quantities in a more efficient manner than a boost-only motor. The maximum final speed and the minimum time results indicate that little freedom is available with the one-pulse motor in terms of the flight time. The three-pulse motor produces identical minimum time performance to the two-pulse motor. Thus, only the two-pulse motor is evaluated. The missile trajectory and motor parameters were optimized so as to maximize the final speed subject to a series of maximum flight-time constraints. These constraints ranged from the minimal flight time of 61.1 s to the maximum final speed flight time of 75.1 s. The resulting parameters are given in Table 11. The final values are given in Table 12.

The results indicate that most of the flight-time control comes from variation in the ignition delay of the second pulse. The fuel allocation between the pulses remains relatively constant. This is an important observation from a practical stand-

Table 12 Final values for t_f constrained maximum final speed trajectories

	t_f constraint (s)					
	Open	70	67	65	63	Min t_f
Speed (ft/s)	2500	2480	2451	2421	2363	2123
Avg. speed (ft/s)	1598	1714	1791	1846	1905	1966
Path angle (deg)	−2.3	−2.2	−2.0	−1.9	−1.4	7.0

point. The fuel allocation in the motor design must be selected in the design, but the ignition delay can be selected in flight. Thus, a near-optimal tradeoff in the final speed and flight time can be controlled by the flight software.

Conclusions

The parameter optimization approach was used to determine the optimal fuel loadout and trajectories for pulse motor designs for maximum final speed, minimal flight time, and maximum final speed with a maximum flight-time constraint. For the horizontal flight maximum final speed problem, performance improved with additional pulses. The three-pulse motor was able to match the final speed of the continuously throttleable ideal boost-sustain motor. A pulse ignition law to maximize the final speed for horizontal flight was found to show exact agreement with the ignition times of this study.

For the horizontal minimal flight-time problem, the performance improved with increased number of pulses. A pulse ignition law for time-minimal flight reproduced the pulse ignition times determined in this study, but robustness remains a concern.

The vertical plane flight results indicate a limited usefulness for the three-pulse motor configuration. For maximizing the final speed at a target, the multiple-pulse motors produced superior results, but the three-pulse motor had significant practical drawbacks. For minimum time flight to a target point, the two-pulse motor is superior to the boost-only motor with the three-pulse motor duplicating the two-pulse trajectory performance. It was found that a fixed two-pulse motor with a variable ignition delay could provide a practical means of exchanging final and average speed in a near-optimal fashion.

Appendix: Airframe Details

The missile used in this study is a single-stage, solid-fuel, planar-wing surface-to-air missile with cruciform fins. The aerodynamic data are given in Ref. 13. The center of gravity was assumed to be located at a total-length-normalized value of 0.51 from the nose tip. A maximum fin deflection of 40 deg was assumed in computing the maximum lift coefficient as a function of Mach number.

The missile airframe and propulsion data are given in Table A1. The specific impulse is representative of a modern missile with some degradation to account for the use of inert materials for the pulse motor.

Table A1 Airframe parameters

Specific impulse (s)	220.7
Exhaust area (ft^2)	0.545
Sea level thrust (lb)	7100.0
Reference area (ft^2)	0.545

Acknowledgment

E. M. Cliff, F. H. Lutze, and H. J. Kelley of the Virginia Polytechnic Institute and State University, Blacksburg, Virginia provided guidance on the initial portion of this work as members of the author's thesis committee.

References

[1]Hibbs, A. R., "Optimum Burning Program for Horizontal Flight," *Journal of the American Rocket Society,* Vol. 22, July–Aug. 1952, pp. 206–112.

[2]Bryson, A. E., and Ross, S. E., "Optimum Rocket Trajectories With Aerodynamic Drag," *Jet Propulsion,* July 1958, pp. 465–469.

[3]Calise, A. J., and Nagy, J., "Necessary Conditions for Optimal Pulse Control," AIAA Paper 85–1955, Aug. 1985.

[4]Calise, A. J., and Prasad, J. V. R., "Pulse Motor Control for Maximizing Average Velocity," *Journal of Guidance, Control, and Dynamics,* Vol. 12, No. 2, March–April 1989, pp. 169–174.

[5]Wassom, S. R., and Gunderson, R. W., "Optimal Pulse Motor Control," AIAA Paper 89–0383, Jan. 1989.

[6]Cheng, V. J. L., Menon, P. K. A., Gupta, N. K., and Briggs, M. M., "Reduced Order Pulse Motor Ignition Logic," *Journal of Guidance, Control, and Dynamics,* Vol. 10, No. 4, July–Aug. 1987, pp. 343–350.

[7]Mennon, P.K.A., Cheng, V. H. L., Lin, C. A., and Briggs, M. M., "High Performance Missile Synthesis with Trajectory and Propulsion System Optimization," *Journal of Spacecraft,* Vol. 24, No. 6, Nov.–Dec. 1987, pp. 552–557.

[8]Baron, R. L., and Abbot, D. W., "Use of Polynomial Networks in Optimum, Real-Time, Two Point Boundary Value Guidance of Tactical Weapons," Military Computing Conference, Military Computing Institute, San Diego, CA, May 3–5, 1988.

[9]Kelley, H. J., "Method of Gradients," *Optimization Techniques,* edited by G. Leitmann, Academic Press, New York, 1962, pp. 205–254.

[10]Kelley, H. J., and Speyer, J. L., "Accelerated Gradient Projection," *Lecture Notes in Mathematics 132,* Springer-Verlag, Berlin, 1970.

[11]Fletcher, R., "A New Approach to Variable Metric Algorithms," *Computer Journal,* Vol. 13, No. 3, pp. 317–326.

[12]Hargraves, C. R., and Paris, S. W., "Direct Trajectory Optimization Using Nonlinear Programming and Collocation," *Journal of Guidance, Control, and Dynamics,* Vol. 10, No. 4, July–Aug. 1987, pp. 338–342.

[13]Corlett, W. A., "Supersonic Stability and Control Characteristics of a Cruciform Missile Model with Delta Wings and Aft Tail Fin Control," NASA TM-80171, 1979.